APL Photonics

Broadband and tunable time-resolved THz system using argon-filled hollow-core photonic crystal fiber

Cite as: APL Photonics **3**, 111301 (2018); https://doi.org/10.1063/1.5043270
Submitted: 07 June 2018 • Accepted: 11 August 2018 • Published Online: 07 September 2018

Wei Cui, Aidan W. Schiff-Kearn, Emily Zhang, et al.

Broadband and tunable time-resolved THz system using argon-filled hollow-core photonic crystal fiber

Wei Cui,[1,2] Aidan W. Schiff-Kearn,[1,2] Emily Zhang,[1,2] Nicolas Couture,[1,2] Francesco Tani,[2,3] David Novoa,[2,3] Philip St.J. Russell,[2,3] and Jean-Michel Ménard[1,2]

[1]*Department of Physics, University of Ottawa, Ottawa, Ontario K1N 6N5, Canada*
[2]*Max Planck Centre for Extreme and Quantum Photonics, Ottawa, Ontario K1N 6N5, Canada*
[3]*Max Planck Institute for the Science of Light, Erlangen 91058, Germany*

(Received 7 June 2018; accepted 11 August 2018; published online 7 September 2018)

We demonstrate broadband, frequency-tunable, phase-locked terahertz (THz) generation and detection based on difference frequency mixing of temporally and spectrally structured near-infrared (NIR) pulses. The pulses are prepared in a gas-filled hollow-core photonic crystal fiber (HC-PCF), whose linear and nonlinear optical properties can be adjusted by tuning the gas pressure. This permits optimization of both the spectral broadening of the pulses due to self-phase modulation (SPM) and the generated THz spectrum. The properties of the prepared pulses, measured at several different argon gas pressures, agree well with the results of numerical modeling. Using these pulses, we perform difference frequency generation in a standard time-resolved THz scheme. As the argon pressure is gradually increased from 0 to 10 bar, the NIR pulses spectrally broaden from 3.5 to 8.7 THz, while the measured THz bandwidth increases correspondingly from 2.3 to 4.5 THz. At 10 bar, the THz spectrum extends to 6 THz, limited only by the spectral bandwidth of our time-resolved detection scheme. Interestingly, SPM in the HC-PCF produces asymmetric spectral broadening that may be used to enhance the generation of selected THz frequencies. This scheme, based on a HC-PCF pulse shaper, holds great promise for broadband time-domain spectroscopy in the THz, enabling the use of compact and stable ultrafast laser sources with relatively narrow linewidths (<4 THz). https://doi.org/10.1063/1.5043270

I. INTRODUCTION

Terahertz time-domain spectroscopy (THz-TDS) is a broadband optical characterization technique increasingly applied in many fields for non-invasive imaging and identification of molecules.[1–8] In condensed matter research, this technique is also used to trace ultrafast dynamics of low-energy excitations when combined with a pump pulse to excite non-equilibrium states inside materials such as semiconductors, strongly correlated materials, superconductors, and topological insulators.[8–18] Common THz-TDS systems, including most of the ones commercially available, are now able to resolve with great sensitivity the spectral range covering 0.5–4 THz. One of the next frontiers in THz photonics is therefore the development of efficient schemes for expanding this spectral window beyond 4 THz, so as to allow access to both a wider range of molecular resonances for sensing applications and new microscopic interactions in condensed matter. Some experimental schemes have already been reported for achieving ultra-broadband THz spectroscopy. They are based on nonlinear optical generation and detection in laser-induced gas plasmas (THz wave air photonics),[19–22] GaP or several-micron-thick ZnTe crystals[23–25] and birefringent $LiGaS_2$ (LGS),[26,27] GaSe,[27–31] and organic crystals such as DAST.[32,33] Although these configurations rely on different types of nonlinear media, they all share an essential common component: an ultrafast near-infrared (NIR) laser capable of delivering broadband femtosecond pulses. Such an optical source is crucial for accessing the high

THz frequency range since THz radiation is generated by nonlinear difference frequency mixing of NIR pulses, which means that the highest generated THz frequencies are determined by the spectral bandwidth of the NIR pulses. Furthermore, efficient time-resolved THz detection requires ultrashort NIR pulses with a duration shorter than the oscillation cycle of the highest THz frequency components to achieve broadband detection. These two conditions impose stringent requirements on the NIR ultrafast source. As a result, expensive and bulky optical systems are often necessary for broadband THz-TDS. We propose an alternative setup for generating broadband THz radiation, one that can be used with a compact and stable MHz laser system delivering pulses of sub-microjoule energy and a few hundreds of femtoseconds in duration. We use a commercial Yb:KGW ultrafast amplifier in combination with a gas-filled kagomé-type hollow-core photonic crystal fiber (kagomé-PCF) to achieve efficient broadband THz generation and detection.[34] Gas-filled hollow-core photonic crystal fiber (HC-PCF) is one of the most efficient and versatile nonlinear platforms for spectral and temporal structuring of NIR pulses.[35–39] It provides weak anomalous dispersion that can be counter-balanced by the normal dispersion of the gas filling the fiber, allowing propagation of ultrashort pulses with minimal temporal distortion. In contrast to solid-core fibers or highly nonlinear materials, the linear and nonlinear properties of the system can be adjusted simply by changing the species and the pressure of the gas filling the HC-PCF. Here, we take advantage of this unique feature to broaden the spectrum covered by the THz-TDS system out to ~6 THz, limited only by the choice of the nonlinear crystal for time-resolved detection. More importantly, the general concept of using a HC-PCF pulse shaper in combination with a relatively narrow spectral linewidth (<4 THz) laser could be extended to other schemes based on different generation and detection crystals such as LGS or GaSe, which would extend further the spectral coverage of THz-TDS.

II. EXPERIMENT AND NUMERICAL SIMULATIONS

The experimental configuration is sketched in Fig. 1. The optical source is a commercial Yb:KGW amplifier delivering 185 fs pulses at a central wavelength of 1035 nm, an average power of 1 W, and a repetition rate of 1.1 MHz. The emitted pulses are launched into an Ar-filled HC-PCF with 75% coupling efficiency. The fiber, a 55 cm-long kagomé-PCF with a 34 μm-diameter core, is entirely placed inside a gas cell within which the Ar pressure can easily be adjusted. This scheme allows us to change the properties of the optical medium and tune the effects of self-phase modulation (SPM) broadening and restructuring the NIR pulse spectrum. A pair of identical chirped mirrors (CMs), providing a total dispersion of -2500 fs^2, is placed after the HC-PCF to compensate for the positive chirp resulting from SPM and to ensure that the pulses are nearly Fourier-transform-limited. A standard THz-TDS configuration is then used to generate and detect the THz radiation.[35] Briefly, the NIR beam is split into two paths. In the first path, phase-locked THz radiation is generated by difference frequency mixing inside a 220 μm thick 110-oriented GaP crystal. The second path is used as an optical gate for time-resolved electro-optical detection. An identical GaP nonlinear crystal is used for detection.

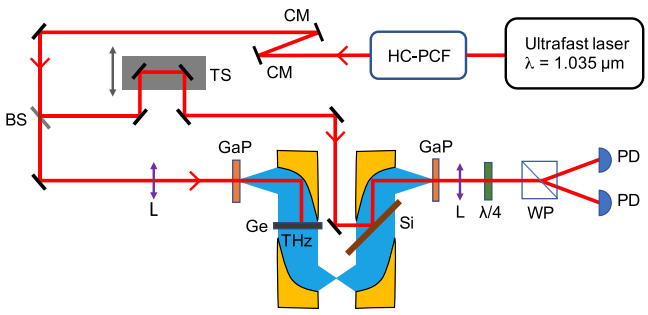

FIG. 1. Schematic of the experimental setup. NIR pulses are launched into a HC-PCF filled with Ar gas at an adjustable pressure. A standard THz-TDS scheme is then used to generate and detect THz radiation.[40] CM: chirped mirror; BS: beam splitter; TS: translational stage; L: lens, GaP: 110-oriented 220 μm-thick gallium phosphide crystal; Ge: germanium wafer; Si: silicon wafer; $\lambda/4$: quarter-wave plate; WP: Wollaston prism; PD: photodetector.

A. Near-infrared pulse propagation in the HC-PCF pulse shaper

The NIR pulse properties are measured after the CMs using a USB spectrometer and a home-made autocorrelator based on second harmonic generation in a 150-μm-thick beta-barium borate (BBO) crystal. As the Ar pressure (P_{Ar}) is increased from 0 to 10 bar, the NIR spectrum gradually broadens from a full-width at half-maximum (FWHM) of 3.5 to 8.7 THz [Fig. 2(a)]. The spectral broadening manifests itself mainly in two sidelobes separated by $\Delta\nu_{SL}$ = 3.1 THz at 7.5 bar and 4.7 THz at 10 bar. The corresponding autocorrelation traces are shown in Fig. 2(b) from which, assuming that the structured NIR pulses have a sech^2 temporal shape, the original pulse duration can be recovered. The pulse duration is observed to decrease gradually, from 185 fs to 65 fs (FWHM), as P_{Ar} is increased. The fact that the spectral bandwidth increases by a factor of 2.5 while the temporal duration decreases by 2.8 indicates that the pulses are close to Fourier-transform-limited at all the pressures used in the experiment.

Figure 2(c) shows the simulated spectra at the fiber output at different Ar pressures for a 185 fs (FWHM) Gaussian pulse with 0.85 μJ energy. The simulations are based on a unidirectional field equation[41] and approximate the fiber dispersion by that of a narrow-bore capillary.[42] Over the pressure range used, the NIR pulses lie in the anomalous dispersion range within the fiber. For these spectral bandwidths, however, the fiber dispersion is insufficient to compensate for the positive chirp resulting from SPM, which therefore requires further compensation using negatively chirped mirrors after the fiber. Figure 2(d) shows the simulated temporal profiles at the fiber output after introducing 2000 fs^2 negative chirp (as in the experiment). As the argon pressure increases from 0 to 10 bar the temporal FWHM decreases from 189 fs to 68 fs, which is in excellent agreement with the experiments. The simulations show no contribution related to pulse-induced gas ionization over the range of parameters used in the experiments.

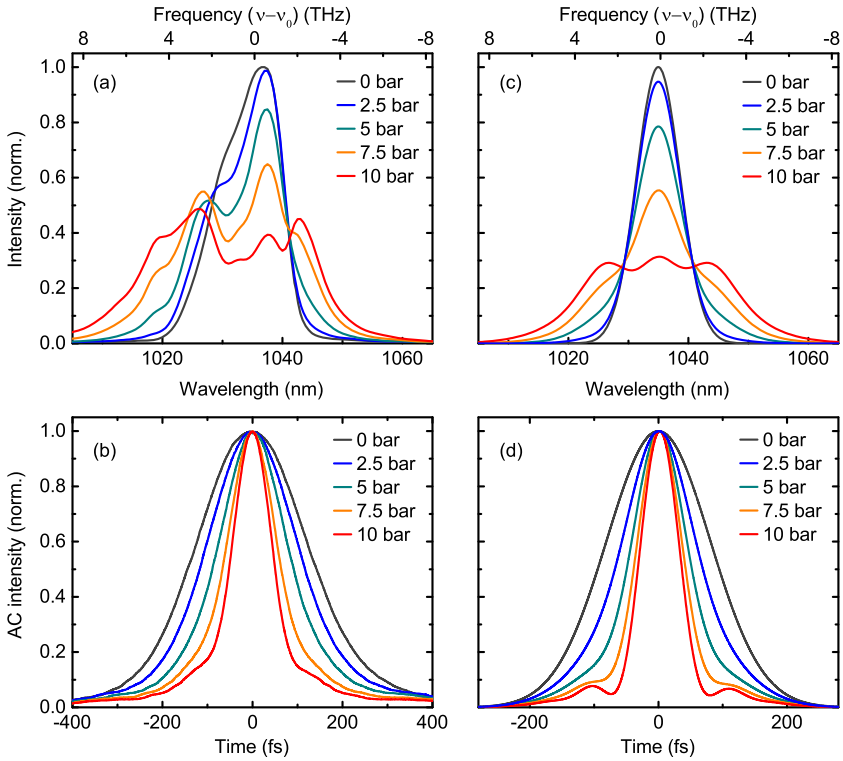

FIG. 2. (a) Spectra of the NIR pulses measured after the HC-PCF and the CM pair for different Ar pressures. (b) Corresponding autocorrelation traces. The FWHM durations measured at P_{Ar} = 0, 2.5, 5, 7.5, and 10 bar are 185, 150, 115, 85, and 65 fs, respectively. [(c) and (d)] For the same conditions, the numerical simulations[41] of the pulse spectra and duration show good agreement with the experiments.

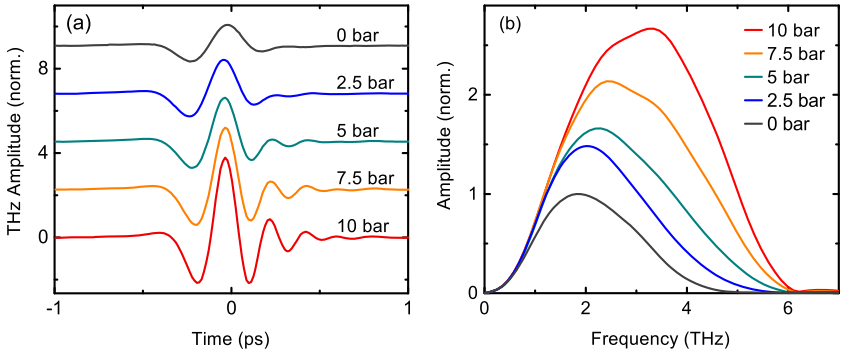

FIG. 3. (a) Phase-locked THz transients measured with NIR pulses prepared in the HC-PCF at different Ar pressures, as shown in Fig. 2. (b) Corresponding THz spectral amplitude calculated by Fourier transforming. In (a) and (b), the maximum amplitude of the measurement at 0 bar is normalized to 1.

B. Phase-locked THz generation

The NIR pulses measured in Figs. 2(a) and 2(b) are injected in the THz-TDS scheme for phase-locked THz generation and detection by electro-optic sampling. Figure 3(a) shows the resulting time-resolved THz field. Simply by adjusting the gas pressure, the peak THz amplitude can be increased by a factor of ~4. This increase is caused by temporal compression of the NIR pulses, leading to higher peak powers and, consequently, to more efficient nonlinear frequency down-conversion. The corresponding THz spectral amplitudes are shown in Fig. 3(b). Distinctly different behavior is observed above and below a frequency of 1 THz: the amplitude of higher spectral components is enhanced as P_{Ar} is increased, while no significant change is observed in the sub-1-THz portion of the spectrum. As a result, the THz bandwidth can be increased from 2.3 THz to 4.5 THz (FWHM). The sudden drop in the spectral amplitude at 6.2 THz is related to the restricted phase-matching conditions in the two 220 μm-thick GaP crystals used for THz generation and detection, which ultimately limit the attainable THz bandwidth. The results agree well with the calculated phase-matching cut-off frequency at 6.6 THz.[43]

Interestingly, SPM in kagomé-PCF produces an unevenly distributed spectrum in the NIR pulses, which will have a direct impact on the generated THz spectrum. At $P_{Ar} > 5$ bar the NIR spectrum departs from a Gaussian-like distribution, displaying two side-lobes separated by $\Delta\nu_{SL}$. Since the THz radiation is produced by difference frequency mixing between NIR pulse components, these side-lobes are expected to enhance THz generation around $\Delta\nu_{SL}$, resulting in distinct peaks in the spectra. However, in the experiment, the electro-optic detection process prevents us from clearly distinguishing this peak since the detection efficiency is not homogeneous over the whole spectral bandwidth.[44,45] Due to the time-resolved configuration, the amplitude of the lowest and highest THz frequencies is under-estimated: Low frequencies have a larger spot size on the detection crystal and do not overlap as well with the focused gating pulse, while high THz frequencies suffer from a phase mismatch with the gating pulse inside the detection crystal. The peak in the measured THz spectra is therefore mostly determined by the time-resolved detection response rather than the spectral shape of the generated THz radiation.

III. CONCLUSION

A pressure-tunable pulse shaper based on gas-filled kagomé-PCF can be used to prepare NIR pulses for efficient broadband THz-TDS. As the Ar pressure is increased in the PCF, spectral broadening and temporal compression of the NIR pulses allow the bandwidth of the measured THz spectrum to be broadened by a factor of 2, the highest frequency component at ~6 THz being limited only by phase-matching conditions in the experiment. This scheme could also be used for accessing higher THz frequencies if the argon pressure is increased beyond 10 bar and different nonlinear generation and detection crystals are used, such as GaSe, LGS, DAST, or $AgGaS_2$. In brief, a single fiber-based module, combined with an ultrafast source with relatively narrow linewidth (<4 THz), can be used

for broadband THz-TDS, paving the way to the design of more compact and cost-effective THz-TDS setups capable of reaching high THz frequencies without the need for complex optical sources based on ultrashort Ti-sapphire amplifiers, synchronized fiber lasers, or optical parametric chirped-pulse amplifiers. Since HC-PCFs are robust and able to guide extremely high peak powers, they may also enable the use of high power and high repetition rate lasers for THz-TDS.[46,47]

ACKNOWLEDGMENTS

J.-M. Ménard acknowledges support from the National Sciences and Engineering Research Council (NSERC), Canada foundation for innovation (CFI), and Ministry of Research and Innovation's (MRI) Ontario Research Fund.

[1] P. Daukantas, "Cultural artifacts in terahertz light," Opt. Photonics News **29**, 28–35 (2018).
[2] C. Seco-Martorell, V. López-Domínguez, G. Arauz-Garofalo, A. Redo-Sanchez, J. Palacios, and J. Tejada, "Goya's artwork imaging with terahertz waves," Opt. Express **21**, 17800–17805 (2013).
[3] A. Redo-Sanchez, B. Heshmat, A. Aghasi, S. Naqvi, M. Zhang, J. Romberg, and R. Raskar, "Terahertz time-gated spectral imaging for content extraction through layered structures," Nat. Commun. **7**, 12665 (2016).
[4] J. F. Federici, B. Schulkin, F. Huang, D. Gary, R. Barat, F. Oliveira, and D. Zimdars, "THz imaging and sensing for security applications—Explosives, weapons and drugs," Semicond. Sci. Technol. **20**, S266 (2005).
[5] B. Fischer, M. Hoffmann, H. Helm, G. Modjesch, and P. U. Jepsen, "Chemical recognition in terahertz time-domain spectroscopy and imaging," Semicond. Sci. Technol. **20**, S246 (2005).
[6] E. P. Parrott and J. A. Zeitler, "Terahertz time-domain and low-frequency Raman spectroscopy of organic materials," Appl. Spectrosc. **69**, 1–25 (2015).
[7] P. D. Cunningham, N. N. Valdes, F. A. Vallejo, L. M. Hayden, B. Polishak, X.-H. Zhou, J. Luo, A. K.-Y. Jen, J. C. Williams, and R. J. Twieg, "Broadband terahertz characterization of the refractive index and absorption of some important polymeric and organic electro-optic materials," J. Appl. Phys. **109**, 043505 (2011).
[8] P. U. Jepsen, D. G. Cooke, and M. Koch, "Terahertz spectroscopy and imaging—Modern techniques and applications," Laser Photonics Rev. **5**, 124–166 (2011).
[9] R. A. Kaindl, M. A. Carnahan, D. Hägele, R. Lövenich, and D. S. Chemla, "Ultrafast terahertz probes of transient conducting and insulating phases in an electron–hole gas," Nature **423**, 734–738 (2003).
[10] R. Huber, F. Tauser, A. Brodschelm, M. Bichler, G. Abstreiter, and A. Leitenstorfer, "How many-particle interactions develop after ultrafast excitation of an electron–hole plasma," Nature **414**, 286–289 (2001).
[11] J.-M. Ménard, C. Poellmann, M. Porer, U. Leierseder, E. Galopin, A. Lemaître, A. Amo, J. Bloch, and R. Huber, "Revealing the dark side of a bright exciton–polariton condensate," Nat. Commun. **5**, 4648 (2014).
[12] M. C. Beard, G. M. Turner, and C. A. Schmuttenmaer, "Transient photoconductivity in GaAs as measured by time-resolved terahertz spectroscopy," Phys. Rev. B **62**, 15764–15777 (2000).
[13] R. Ulbricht, E. Hendry, J. Shan, T. Heinz, and M. Bonn, "Carrier dynamics in semiconductors studied with time-resolved terahertz spectroscopy," Rev. Mod. Phys. **83**, 543–586 (2011).
[14] M. Porer, U. Leierseder, J.-M. Ménard, H. Dachraoui, L. Mouchliadis, I. E. Perakis, U. Heinzmann, J. Demsar, K. Rossnagel, and R. Huber, "Non-thermal separation of electronic and structural orders in a persisting charge density wave," Nat. Mater. **13**, 857–861 (2014).
[15] C. Poellmann, P. Steinleitner, U. Leierseder, P. Nagler, G. Plechinger, M. Porer, R. Bratschitsch, C. Schüller, T. Korn, and R. Huber, "Resonant internal quantum transitions and femtosecond radiative decay of excitons in monolayer WSe_2," Nat. Mater. **14**, 889–893 (2015).
[16] C. J. Docherty, P. Parkinson, H. J. Joyce, M.-H. Chiu, C.-H. Chen, M.-Y. Lee, L.-J. Li, L. M. Herz, and M. B. Johnston, "Ultrafast transient terahertz conductivity of monolayer MoS_2 and WSe_2 grown by chemical vapor deposition," ACS Nano **8**, 11147–11153 (2014).
[17] R. Valdés Aguilar, J. Qi, M. Brahlek, N. Bansal, A. Azad, J. Bowlan, S. Oh, A. J. Taylor, R. P. Prasankumar, and D. A. Yarotski, "Time-resolved terahertz dynamics in thin films of the topological insulator Bi_2Se_3," Appl. Phys. Lett. **106**, 011901 (2015).
[18] L. Junpeng and L. Hongwei, "A critical review on the carrier dynamics in 2D layered materials investigated using THz spectroscopy," Opt. Commun. **406**, 24–35 (2018).
[19] D. J. Cook and R. M. Hochstrasser, "Intense terahertz pulses by four-wave rectification in air," Opt. Lett. **25**, 1210–1212 (2000).
[20] X. Xie, J. Dai, and X.-C. Zhang, "Coherent control of THz wave generation in ambient air," Phys. Rev. Lett. **96**, 075005 (2006).
[21] J. Dai, X. Xie, and X.-C. Zhang, "Detection of broadband terahertz waves with a laser-induced plasma in gases," Phys. Rev. Lett. **97**, 103903 (2006).
[22] E. Matsubara, M. Nagai, and M. Ashida, "Ultrabroadband coherent electric field from far infrared to 200 THz using air plasma induced by 10 fs pulses," Appl. Phys. Lett. **101**, 011105 (2012).
[23] A. Leitenstorfer, S. Hunsche, J. Shah, M. C. Nuss, and W. H. Knox, "Detectors and sources for ultrabroadband electro-optic sampling: Experiment and theory," Appl. Phys. Lett. **74**, 1516 (1999).
[24] K. Aoki, J. Savolainen, and M. Havenith, "Broadband terahertz pulse generation by optical rectification in GaP crystals," Appl. Phys. Lett. **110**, 201103 (2017).
[25] R. Huber, B. Schmid, R. Kaindl, and D. Chemla, "Femtosecond THz studies of intra-excitonic transitions," Phys. Status Solidi B **245**, 1041–1048 (2008).

[26] I. Pupeza, D. Sánchez, J. Zhang, N. Lilienfein, M. Seidel, N. Karpowicz, T. Paasch-Colberg, I. Znakovskaya, M. Pescher, W. Schweinberger, V. Pervak, E. Fill, O. Pronin, Z. Wei, F. Krausz, A. Apolonski, and J. Biegert, "High-power sub-two-cycle mid-infrared pulses at 100 MHz repetition rate," Nat. Photonics **9**, 721 (2015).
[27] M. Knorr, J. Raab, M. Tauer, P. Merkl, D. Peller, E. Wittmann, E. Riedle, C. Lange, and R. Huber, "Phase-locked multi-terahertz electric fields exceeding 13 MV/cm at a 190 kHz repetition rate," Opt. Lett. **42**, 4367–4370 (2017).
[28] C. Kübler, R. Huber, S. Tübel, and A. Leitenstorfer, "Ultrabroadband detection of multi-terahertz field transients with GaSe electro-optic sensors: Approaching the near infrared," Appl. Phys. Lett. **85**, 3360 (2004).
[29] K. Liu, J. Xu, and X.-C. Zhang, "GaSe crystals for broadband terahertz wave detection," Appl. Phys. Lett. **85**, 863 (2004).
[30] A. Sell, A. Leitenstorfer, and R. Huber, "Phase-locked generation and field-resolved detection of widely tunable terahertz pulses with amplitudes exceeding 100 MV/cm," Opt. Lett. **33**, 2767–2769 (2008).
[31] J. Zhang, K. F. Mak, N. Nagl, M. Seidel, D. Bauer, D. Sutter, V. Pervak, F. Krausz, and O. Pronin, "Multi-mW, few-cycle mid-infrared continuum spanning from 500 to 2250 cm^{-1}," Light: Sci. Appl. **7**, 17180 (2018).
[32] H. Adachi, T. Taniuchi, M. Yoshimura, S. Brahadeeswaran, T. Higo, M. Takagi, Y. Mori, T. Sasaki, and H. Nakanishi, "High-quality organic 4-dimethylamino-N-methyl-4-stilbazolium tosylate (DAST) crystals for THz wave generation," Jpn. J. Appl. Phys., Part 2 **43**, L1121 (2004).
[33] M. Martin, J. Mangeney, P. Crozat, and P. Mounaix, "Optical phase detection in a 4-N,N-dimethylamino-4′-N′-methyl-stilbazolium tosylate crystal for terahertz time domain spectroscopy system at 1.55 μm wavelength," Appl. Phys. Lett. **97**, 111112 (2010).
[34] F. Benabid, J. C. Knight, G. Antonopoulos, and P. St. J. Russell, "Stimulated Raman scattering in hydrogen-filled hollow-core photonic crystal fiber," Science **298**, 399–402 (2002).
[35] K. F. Mak, M. Seidel, O. Pronin, M. H. Frosz, A. Abdolvand, V. Pervak, A. Apolonski, F. Krausz, J. C. Travers, and P. St. J. Russell, "Compressing μJ-level pulses from 250 fs to sub-10 fs at 38-MHz repetition rate using two gas-filled hollow-core photonic crystal fiber stages," Opt. Lett. **40**, 1238–1241 (2015).
[36] P. St. J. Russell, P. Hölzer, W. Chang, A. Abdolvand, and J. C. Travers, "Hollow-core photonic crystal fibres for gas-based nonlinear optics," Nat. Photonics **8**, 278–286 (2014).
[37] M. Saleh and F. Biancalana, "Tunable frequency-up/down conversion in gas-filled hollow-core photonic crystal fibers," Opt. Lett. **40**, 4218 (2015).
[38] J. Travers, W. Chang, J. Nold, N. Joly, and P. St. J. Russell, "Ultrafast nonlinear optics in gas-filled hollow-core photonic crystal fibers," J. Opt. Soc. Am. B **28**, A11 (2011).
[39] O. Heckl, C. Saraceno, C. Baer, T. Südmeyer, Y. Wang, Y. Cheng, F. Benabid, and U. Keller, "Temporal pulse compression in a xenon-filled Kagome-type hollow-core photonic crystal fiber at high average power," Opt. Express **19**, 19142 (2011).
[40] X.-C. Zhang and J. Xu, *Introduction to THz Wave Photonics* (Springer, 2010).
[41] F. Tani, J. C. Travers, and P. St.J. Russell, "Multimode ultrafast nonlinear optics in optical waveguides: Numerical modeling and experiments in kagomé photonic-crystal fiber," J. Opt. Soc. Am. B **31**, 311–320 (2014).
[42] E. A. J. Marcatili and R. A. Schmeltzer, "Hollow metallic and dielectric waveguides for long distance optical transmission and lasers," Bell Syst. Tech. J. **43**, 1783–1809 (1964).
[43] D. R. Parsons and P. D. Coleman, "Far infrared optical constants of gallium phosphide," Appl. Opt. **10**, 1683–1685 (1971).
[44] G. Gallot and D. Grischkowsky, "Electro-optic detection of terahertz radiation," J. Opt. Soc. Am. B **16**, 1204–1212 (1999).
[45] A. Tomasino, A. Parisi, S. Stivala, P. Livreri, A. C. Cino, A. C. Busacca, M. Peccianti, and R. Morandotti, "Wideband THz time domain spectroscopy based on optical rectification and electro-optic sampling," Sci. Rep. **3**, 3116 (2013).
[46] F. Emaury, C. J. Saraceno, B. Debord, D. Ghosh, A. Diebold, F. Gerome, T. Sudmeyer, F. Benabid, and U. Keller, "Efficient spectral broadening in the 100-W average power regime using gas-filled kagomé HC-PCF and pulse compression," Opt. Lett. **39**, 6843–6846 (2014).
[47] U. Elu, M. Baudisch, H. Pires, F. Tani, M. H. Frosz, F. Köttig, Al. Ermolov, P. St.J. Russell, and J. Biegert, "High average power and single-cycle pulses from a mid-IR optical parametric chirped pulse amplifier," Optica **4**, 1024–1029 (2017).